Application Note 42

Raman Microspectrometer

Technology and Applications Center
Newport Corporation

Spectra-Physics
A Division of Newport Corporation

Newport
Experience | Solutions

Introduction:

Raman scattering was discovered by Sir C. V. Raman[1,2] in the 1920's. Since then Raman spectroscopy has become one of the most popular analytical techniques. It provides comprehensive information about the vibrational modes of molecules by monitoring macroscopic light scattering and has created an entire new branch of molecular spectroscopy. The Raman scattered light from the molecules, frequency shifted relative to the frequency of the light source, is generally polarized and contains information about the vibrational frequencies and anisotropy of molecular vibrations. As is well known, vibrational modes are like fingerprints of molecules. Therefore, Raman scattering is endowed with the sensitivity to discern different molecular species. Raman spectroscopy has broad applications, ranging from fundamental physical chemistry, inorganic chemistry, biochemistry, art and archaeology, to highly practical forensic examinations[3].

Unlike Rayleigh scattering, where the scattered light has the same frequency and strong signal relative to the excitation, Raman scattering is frequency shifted and extremely weak (about one photon out of 10^9 ~ 10^{11} impinging photons is scattered). As Raman himself pointed out, "the chief difficulty which had oppressed us in the study of the new phenomenon (Raman scattering) was its extreme feebleness in general"[4]; increasing the sensitivity, resolution and ease of use of the experimental setups are of prime interest. After the first experiments done by Raman, significant advances over the years in light sources (monochromic laser sources vs. sunlight), filters (varieties of dichroic filters vs. glass filters) and detectors (CCD cameras, etc. vs. photographic films) boosted the feasibility and popularity of this technique. It is important to point out that the resolution of the Raman scattering is determined by the bandwidth of the light source and the resolution of the spectrometer, while the sensitivity threshold is mainly defined by the optics and detectors being employed.

Another technique related to vibrational spectroscopy, Fourier Transformed Infrared Spectroscopy (FTIR), is often compared with Raman scattering. In fact, the two techniques complement each other. Approximately, a vibrational mode would be infrared active if the vibration causes the change of the molecule's dipole moment. On the other hand, it would be Raman active if the vibration induces the change of the molecule's polarizability[5]. Experimentally, Raman spectroscopy is favored by researchers because the components for the spectrometer are readily available and the entire setup can be situated in open air. On the contrary, a FTIR spectrometer includes a wide radiation spectrum lamp, purging system, motorized translation stages, temperature controlled semiconductor detectors (TE cooled InGaAs detector for instance) and a mathematical algorithm to deconvolve the interferogram. It is therefore not cost efficient and discourages researchers from building it from the bottom up. Consequently, commercial FTIR systems are frequently shared by researchers. One concern with Raman scattering that must be controlled is the potential background fluorescence from the samples while FTIR has interferences from water vapor and CO_2 that must be removed via purge or background subtraction.

In this application note, we present the theory of Raman scattering, describe a simple and easy-to-implement experimental Raman setup, and show the results on several liquids and some organic compounds to exemplify the sensitivity and resolution of the system.

Theory

A classical treatment is presented here to elucidate the essential phenomena of Raman scattering[5]. To begin with, notice that the scattered field $\tilde{E}_S(t)$ originates from the induced oscillatory polarization $\tilde{P}_S(t)$ of the sample after the interaction with the input field, $\tilde{E}_i(t)$. It can be expressed as:

$$\tilde{E}_s(t) \propto \tilde{P}_s(t) = \hat{a} \cdot \tilde{E}_i(t) \Rightarrow \begin{pmatrix} \tilde{E}_{S,X}(t) \\ \tilde{E}_{S,Y}(t) \\ \tilde{E}_{S,Z}(t) \end{pmatrix} = \begin{pmatrix} a_{XX}\, a_{XY}\, a_{XZ} \\ a_{YX}\, a_{YY}\, a_{YZ} \\ a_{ZX}\, a_{ZY}\, a_{ZZ} \end{pmatrix} \begin{pmatrix} \tilde{E}_{i,X}(t) \\ \tilde{E}_{i,Y}(t) \\ \tilde{E}_{i,Z}(t) \end{pmatrix}; \quad (1)$$

where $\hat{a}$ is the polarizability tensor of the molecule, and X, Y, Z is the lab reference coordinate system. $\hat{a}$ is a function of electron clouds and nuclei of the molecule and is influenced by the molecular vibrations. Considering a vibrational mode specified by the normal coordinate, Q_k, $\hat{a}$ can be expanded as:

$$\hat{a} = \hat{a}^o + \left(\frac{\partial \hat{a}}{\partial Q_k}\right)_o \cdot Q_k + \left(\frac{\partial^2 \hat{a}}{\partial Q_k^{\,2}}\right)_o : Q_k^{\,2} + \text{higher order terms}; \quad (2)$$

Equation (2) shows that the displacement of the vibration directly influences the polarizability. In addition, the vibration of a mode and the input field can be expressed as:

$$Q_k = Q^o_k \cos(\omega_k t);\ \tilde{E}_i(t) = E_i^o \cos(\omega t); \quad (3)$$

In equation (3), ω_k is the vibrational frequency and ω is the frequency of the light source. Substituting (3) and (2) into (1), we arrive at:

$$\tilde{E}_{s,X}(t) \propto P_{s,X}(t) = \sum_{n=X,Y,Z} a_{Xn} \tilde{E}_{i,n}(t) = \overbrace{a^o_{XX} E^o_{iX} \cos(\omega t)}^{(a)} + \overbrace{\left(\frac{\partial a_{XX}}{\partial Q_k}\right)_o \cdot Q^o_k \cos(\omega_k t) E^o_{iX} \cos(\omega t) + \ldots}^{(b)} \quad (4)$$

Using the trigonometric identity,

$\cos(\alpha)\cos(\beta) = \frac{1}{2}[\cos(\alpha-\beta)+\cos(\alpha+\beta)]$, part (b) in equation (4) can be expressed:

$$(b) = \frac{1}{2}\left(\frac{\partial a_{XX}}{\partial Q_k}\right)_o \cdot Q^o_k E^o_{iX} [\cos(\omega+\omega_k)t + \cos(\omega-\omega_k)t]\ ; \quad (5)$$

According to (a) of (4), part of the scattered light has the same frequency as the light source and is referred to as Rayleigh scattering. On the other hand, (b) contains the frequencies of $\omega + \omega_k$ and $\omega - \omega_k$ and are called anti-Stokes Raman and Stokes Raman scattering, respectively. Therefore, by measuring the frequencies of the scattered light, we would be able to infer the frequencies of the molecular vibrational modes. From (2) we can also see that under the first order approximation, the vibration would be Raman active if the derivative of the polarizability is not zero.

Experimental Setup

The setup is based on a 532 nm CW single frequency DPSS laser (Excelsior®, Spectra-Physics) as the light source. Lasers with longer wavelengths are more preferable in Raman experiments since some of the fluorescence can be avoided. For example, Newport's 785nm Raman Laser Module, would be an appropriate choice. Figure 1 shows the homebuilt Raman microspectrometer system used in Newport's Technology & Application Center (TAC). The laser beam passes through a variable attenuator (application note 26) used to control the laser intensity. Then the beam is routed into a 45° dichroic beamsplitter. The beamsplitter has to be set exactly at 45° to the incident beam in order to maximize the reflection of the light source into the sample and transmission of the Raman scattered signal, as well as minimize the transmission of the back-reflected laser beam. Without employing a microscope at this stage, the laser beam can be focused by a simple lens into the sample situated on XYZ stages. In the setup described in this application note, the laser beam is routed into a microscope and then focused in the sample by an objective. The sample is held on the XY observation platform of the microscope and the focal point is controlled by adjusting the height of the objective.

The scattered Raman light is collimated by the objective/lens and all wavelengths longer than the light source are passed through the same 45° dichroic beamsplitter. Most residual source light is cut off at this point. After passing through this filter, the beam is routed and focused on the entrance slit of a spectrometer by a condenser lens. This lens is situated on a stage in order to adjust the focal point of the Raman field relative to the entrance slit. A zero degree long wave pass filter is used in front of the entrance slit to block any residual scattered excitation light. The spectrometer is composed of a monochromator (MS260i™ 1/4m Spectrograph) and a CCD camera (InstaSpec® X). The Raman field is dispersed by the monochromator and imaged by the CCD camera.

The fluorescence from a rhodamine dye solution is used to align the spectrometer. The objective/lens collimates the fluorescence and fills the entire apertures of the filter and subsequent routing mirrors. Three metallic mirrors after the filter are used to route the fluorescence light into the spectrometer. The condenser lens on the linear stage focuses it on the entrance slit of the spectrometer. After the alignment procedure, the sample of interest is put on the sample holder. At this point, only small adjustments of the objective/lens, condenser lens, and the last mirror before the condenser lens would be required to maximize the Raman signal.

In the setup we described above, Stokes Raman scattering is measured. By simply modifying the system to use different kinds of filters, the measurements of the anti-Stokes Raman Scattering can also be achieved.

Figures

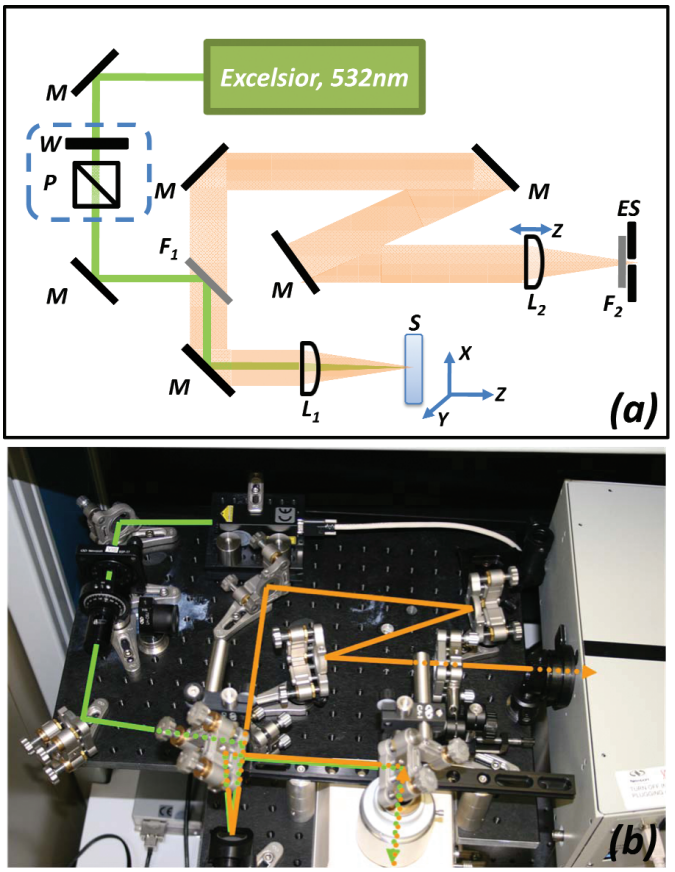

Figure 1. (a) A diagram shows the principle of the experimental setup. M: mirror, W: waveplate, P: polarizer, S: sample, F_1: 45° beamsplitter, F_2: long wave pass filter, L_1: objective or lens, L_2: condenser lens, ES: entrance slit of the spectrometer. The dashed circle marks the attenuator. (b) Photograph of the Raman Microspectrometer setup in the Newport TAC. The laser is shown in green, while the Raman scattered field is shown in orange.

Results

Figure 2 shows the experimental results for several neat solvents. In all of the experiments, the exposure time was less than 20 seconds. In some cases, like with cyclohexane, the measurement can actually be monitored in real time (the

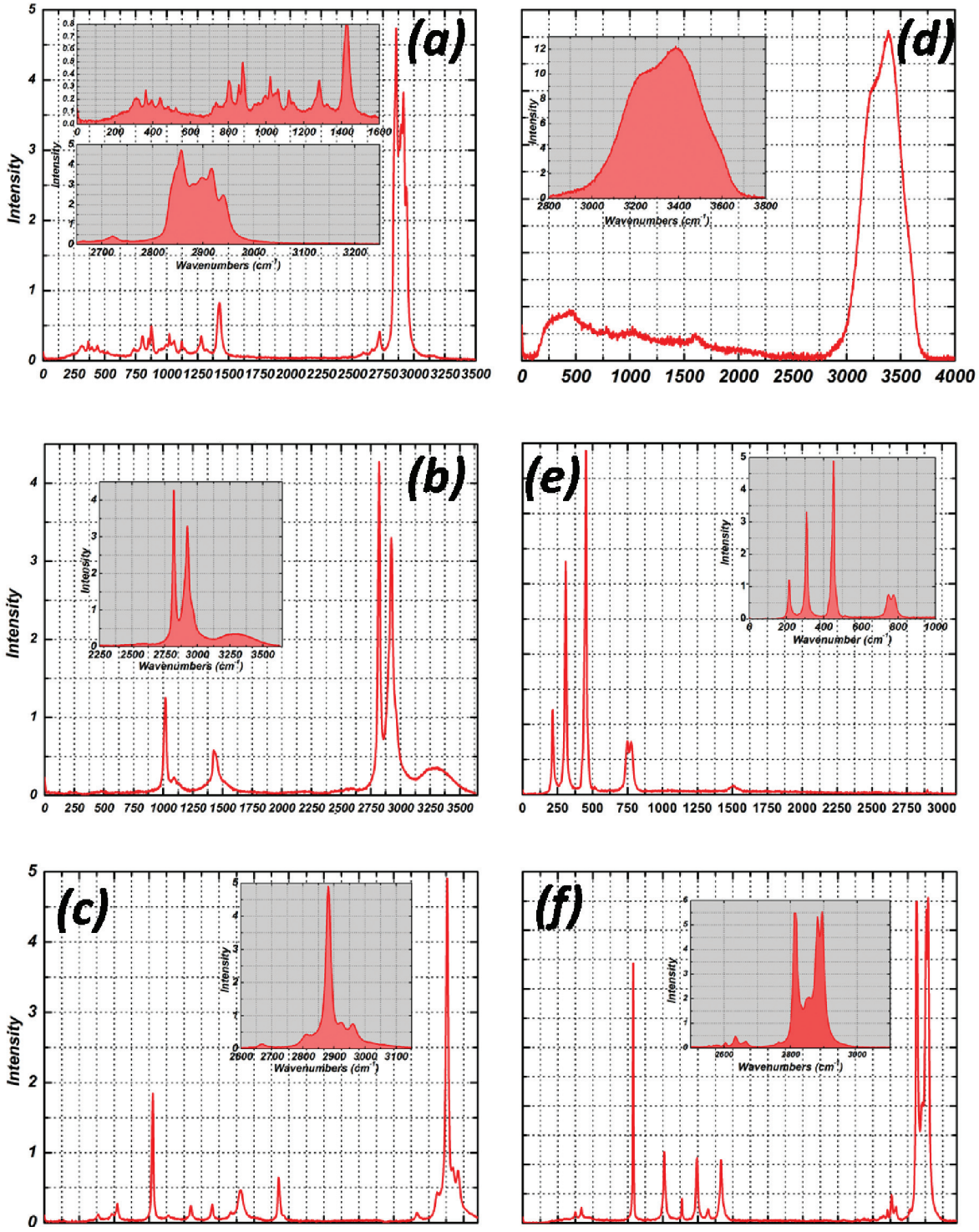

Figure 2. Raman spectra of n-hexane (a), methanol (b), acetone (c), water (d), carbon tetrachloride (e), cyclohexane (f). The inset of each spectrum shows the region where the peaks are most congested.

frame was updated every second and the result is satisfactory). Even in the highly congested parts of the spectra, such as fingerprint regions of hexane (inset of figure 2(a)) or C-H stretch regions of n-hexane, cyclohexane, and acetone (figures 2(a), (c) and (f)), the spectra are well resolved. By comparing the spectra, a resolution better than 3 cm^{-1} is achieved. The flat baselines in figure 2 are an indication of excellent signal-to-noise ratio. As shown in the low frequency region of figure 2(d), this cutoff frequency occurs at about 180 cm^{-1}, making the study of low vibrational modes feasible. The presented results demonstrate the high sensitivity and resolution of this simple setup.

In the next example, we recorded Raman spectra of ethyl acrylate and ethyl propionate. The geometries of these molecules are similar, however, ethyl acrylate has conjugated double bonds (carbonyl and C-C double bond) while propionate has only the carbonyl group. Figure 3(a) shows their molecular structures for comparison. We dissolved both chemicals in carbon tetrachloride and the results are shown in figure 3(b). As can be seen from figure 3(b), the Raman spectra of these two chemicals are very different despite their similar molecular structures. The biggest discrepancy occurs in the frequency region between 1600 and 1800 cm^{-1}. This region contains the vibrational modes that involve stretching of double bonds. For ethyl acrylate, there are two vibrations (in-phase and out-of-phase double bonds stretches, as shown on the inset of figure 3(b)). For ethyl propionate, there is only one vibration involving the stretch of the carbonyl group. In addition, the Raman intensities of these modes of ethyl acrylate are much stronger than that of ethyl propionate. Two main reasons account for this. First of all, in a conjugated system like ethyl acrylate, the electrons are delocalized through π-bonds interaction. In other words, the electrons are less trapped by the nuclei and easily polarized by the electric field. As a result, the polarizability is larger. Secondly, the deformation caused by the vibrational modes of acrylate is larger than that of ethyl propionate since it involves two double bonds. This induces a larger change of the polarizability.

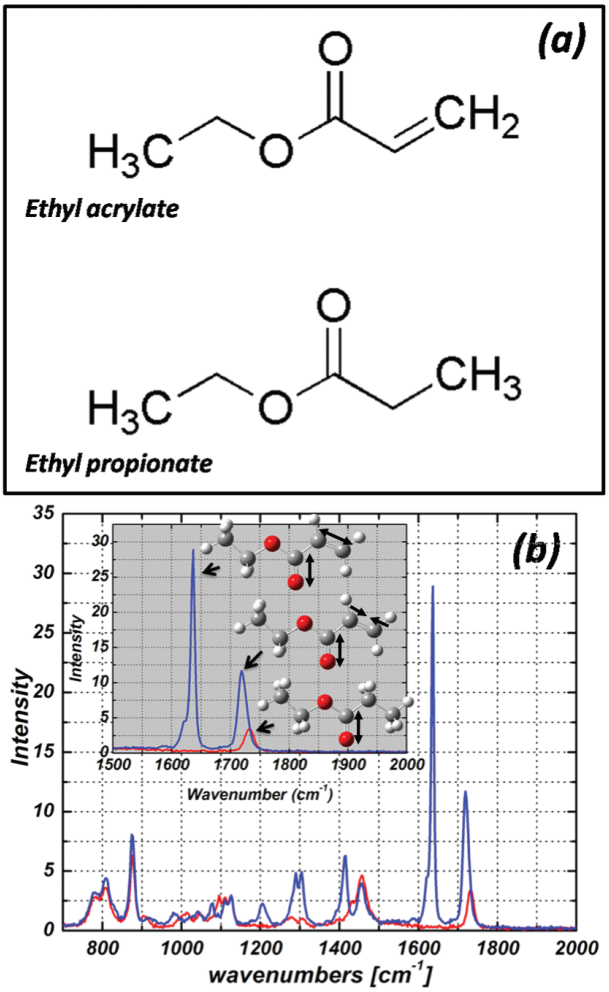

Figure 3. (a) The chemical structures of ethyl acrylate and ethyl propionate. (b) The Raman spectra of ethyl acrylate and ethyl propionate in CCl_4. Blue/red traces are for ethyl acrylate/propionate solution, respectively. The spectra in the 1600 cm^{-1} region are shown in the inset where the dominant displacements of the normal modes are also demonstrated.

Then, we recorded the Raman spectra of two monomers frequently used in photo-polymerization processes (application note 37). They are both triacrylate monomers and named SR-499 and SR-368 (Sartomer Company, Inc., Exton, PA). The molecular structure and the measured Raman spectra are shown in figure 4. SR-499 has a vibrational mode which is related to the carbonyl group and labeled as α, while

SR-368 has two of those modes, β and γ. These vibrations have similar frequencies since the main displacements of these modes involve the stretch of the carbonyl groups. Their Raman spectra are shown in Figure 4(b). They are similar except in the 1700 cm^{-1} frequency region. As shown in the inset of Figure 4(b), two peaks related to the different carbonyl groups of SR-368 are well resolved. Only one peak is observed for SR-499. In addition, α and β have almost the same frequency. All of these results coincide perfectly with predictions from the structures of the molecules.

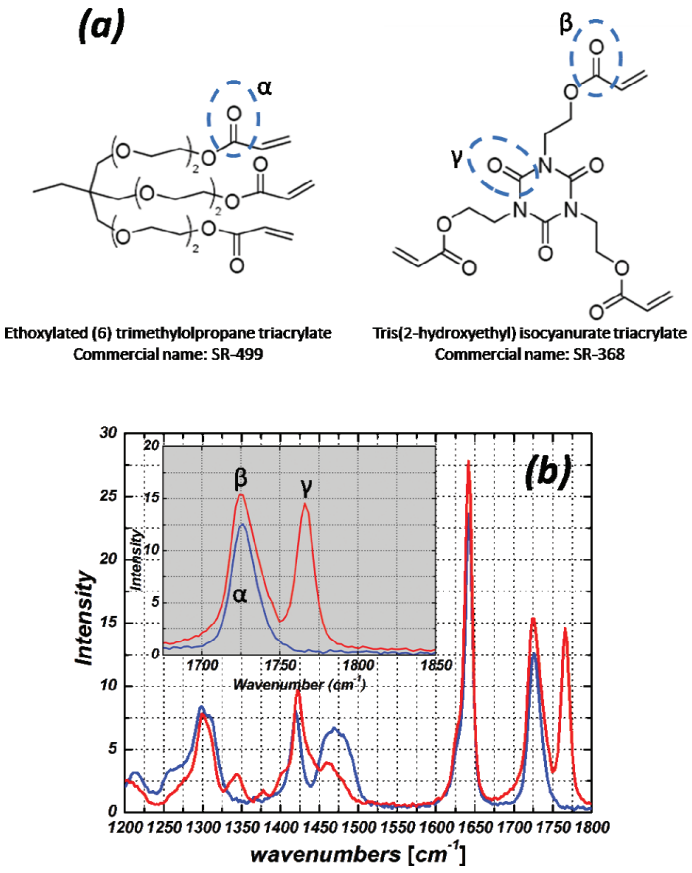

Figure 4. (a) Molecular structures of SR-499 *and* SR-368. *Also shown are the carbonyl groups which contribute to different vibrational modes. (b) Raman spectra of* SR-499 *and* SR-368. *Inset: the* 1700 cm^{-1} *region is magnified to show different vibrational modes of the molecules.*

Conclusion

A homemade Raman spectrometer is presented in this application note. The system is compact, simple and cost-effective. The performance is demonstrated using several chemicals as examples. Excellent sensitivity and resolution are achieved.

References

1. C.V. Raman, and K.S. Krishnan, A New Type of Secondary Radiation. N*ature*, (1928). 121: 501-502.
2. C.V. Raman, A New Radiation. Indian Journal of Physics, (1928). 2: 387.
3. E. Smith and G. Dent, Modern Raman Spectroscopy: A P*ractical A*pproach. (2005).
4. C.V. Raman, The Molecular Scattering of Light. N*obel L*ecture, (1930).
5. D.A. Long, The Raman Effect: A U*nified T*reatment *of the T*heory *of* R*aman S*cattering *by* M*olecules*. (2001).

Newport Corporation

Worldwide Headquarters
1791 Deere Avenue
Irvine, CA 92606

(In U.S.): 800-222-6440
Tel: 949-863-3144
Fax: 949-253-1680

Email: sales@newport.com

Newport
Experience | Solutions

Visit Newport Online at: **www.newport.com**

ISO 9001
FM 27207

Newport Corporation, Irvine, California, has been certified compliant with ISO 9001 by the British Standards Institution.

MM#9000102
DS-04093